Wing flexibility improves bumblebee flight stability

Emily A Mistick[a]

Andrew M Mountcastle[a]

Stacey A Combes[b]

[a]Harvard University, Department of Organismic and Evolutionary Biology, Concord Field Station, 100 Old Causeway Road, Bedford, MA 01730.

[b]University of California, Davis, Department of Neurobiology, Physiology, and Behavior, 1 Shields Avenue, Davis, CA 95616.

Abstract

Insect wings do not contain intrinsic musculature to change shape, but rather bend and twist passively during flight. Some insect wings feature flexible joints along their veins that contain patches of resilin, a rubber-like protein. Bumblebee wings exhibit a central resilin joint (1m-cu) that has previously been shown to improve vertical force production during hovering flight. In this study, we artificially stiffened bumblebee (*Bombus impatiens*) wings *in vivo* by applying a micro-splint to the 1m-cu joint, and measured the consequences for body stability during forward flight in both laminar and turbulent airflow. In laminar flow, bees with stiffened wings exhibited significantly higher mean rotation rates and standard deviation of orientation about the roll axis. Decreasing the wing's flexibility significantly increased its projected surface area relative to the oncoming airflow, likely increasing the drag force it experienced during particular phases of the wingstroke. We hypothesize that higher drag forces on stiffened wings decrease body stability when the left and right wings encounter different flow conditions. Wing splinting also led to a small increase in body rotation rates in turbulent airflow, but this change was not statistically significant, possibly because bees with stiffened wings changed their flight behavior in turbulent flow. Overall, we find that wing flexibility improves flight stability in bumblebees, adding to the growing appreciation that wing flexibility is not merely an inevitable liability in flapping flight, but can enhance flight performance.

Keywords: insect flight, morphology, wing flexibility, turbulence, stability, flapping flight

1. Introduction

Insects are the oldest group of flying animals, and the high energetic cost of flight has likely imposed strong selective pressures on morphological and physiological features associated with flight, such as the wings. Much of our understanding of insect flight aerodynamics has been gained through the use of physical and computational models that approximate wings as rigid, flat plates, because incorporating wing flexibility into such models presents significant challenges. In reality, however, many insect wings are flexible structures, which can undergo significant deformations during flight. These shape changes are entirely passive, as insect wings do not contain intrinsic musculature (Wooton, 1992). Thus, the structural and material properties of a wing determine how it will deform in response to inertial and aerodynamic loads (Daniel and Combes, 2002).

Insect wings consist of a thin, flexible membrane supported by a network of veins with solid, chitin walls. The wing veins of some insects, including dragonflies and bumblebees, feature joints containing small patches of embedded resilin, a highly flexible, rubber-like protein with remarkably high elastic efficiency (Weis-Fogh, 1961). These flexible resilin joints allow wing veins to reversibly deform during collisions (Mountcastle and Combes, 2014) and influence overall wing flexibility and shape changes during flight (Mountcastle and Combes, 2013).

Recently, Mountcastle et al. (2013) developed an experimental technique to stiffen the wings of live insects by splinting individual resilin joints, enabling researchers to directly test the effects of wing flexibility on insect flight performance. Their findings – that wing flexibility enhances vertical aerodynamic force production and thus load lifting capacity (Mountcastle et al. 2013) – are qualitatively consistent with the results of several recent computational studies that have also explored this question (Shyy et al.,

2008; Kim et al., 2009; Young et al 2009, Du and Sun 2010; Nakata and Liu 2011). However, while there has been a recent surge in research activity surrounding the role of wing flexibility in insect flight aerodynamics, nearly all of these studies have focused on relatively simple flight behaviors in still air (i.e., hovering or load lifting). No studies to date have explored how insect wing flexibility may affect other aspects of flight performance beyond force production and aerodynamic efficiency. In this study, we use the vein-joint splinting technique developed by Mountcastle et al. (2013) to test the effects of wing flexibility on flight stability in bumblebees, which we define here as the capacity to maintain constant orientation and heading during steady flight.

There are several potential mechanisms by which wing flexibility may affect flight stability in insects. In birds, steppe eagles actively change the shape of their wings in response to turbulent gusts, decreasing wing area to minimize perturbations caused by aerodynamic drag (Reynolds, 2014). Although insects do not have the same degree of active control over wing shape, wing flexibility may nevertheless serve a similar stabilizing role, by allowing the wing to passively bend out of the way in response to gusts, reducing the asymmetric aerodynamic forces acting on the insect. In addition, wing deformations that naturally arise during the flapping cycle periodically reduce the projected area of the wing with respect to the oncoming airflow, thereby reducing its form drag. If flight instabilities are predominantly caused by unpredictable flow asymmetries between the left and right wings, then increased drag caused by greater projected wing area might amplify the destabilizing effect of a given aerodynamic asymmetry – whether this is due to an unexpected gust of wind or to the insect's own

motions (i.e., asymmetric flapping, body rotations, or non-zero yaw angles relative to the oncoming airflow).

To approximate the wide range of aerial conditions that insects encounter in their natural habitats, and to help tease apart the potential mechanisms by which wing flexibility may affect stability, we performed flight experiments in both smooth and turbulent airflow. Although most experimental insect flight studies are conducted in still air or smooth flow, wild insects typically fly within a few hundred meters of the Earth's surface, in the atmospheric boundary layer (ABL), where wind speed and direction are highly variable. Turbulence arises in the ABL due to interactions between the oncoming airflow and surface features, such as mountains, buildings, and plants (Stull, 1988). As insects move through natural habitats, they must negotiate this range of unpredictable, varying airflow patterns, not only maintaining stable flight, but also carrying out complex flight maneuvers. Bumblebees, for example, engage in long foraging bouts through diverse physical and aerial landscapes, and are often seen foraging in high winds and inclement weather (Heinrich, 2004).

In recent years, a few studies have examined animal flight stability in unsteady, structured airflow, specifically in von Kármán vortex streets – the regular patterns of alternating vortices that are formed immediately downstream of an object in flow (Ravi et al. 2013, Mountcastle et al. 2015, Ortega-Jimenez et al., 2013 and 2014). Bumblebees flying in von Kármán vortex streets display greater fluctuations in body orientation and higher rotation rates than when flying in laminar air, with the greatest instabilities occurring about the roll axis (i.e., rotations around the longitudinal axis of the body; Ravi et al., 2013, Mountcastle et al. 2015). Vortex streets have also been shown to reduce

flight stability in hummingbirds and hawkmoths, and to induce changes in flapping kinematics in some cases (Ortega-Jimenez et al., 2013 and 2014). Although these studies have provided valuable insight into animal flight dynamics in unsteady airflows, these types of structured wakes only occur in limited locations in the natural world (e.g., immediately downstream of an object). Fully mixed, free-stream turbulence, which is characterized by a chaotic blend of vortices spanning a range of sizes, is likely far more common in outdoor habitats.

We examined the effect of wing flexibility on insect flight stability by comparing the forward flight performance of bumblebees with naturally flexible wings and with artificially stiffened wings, in both smooth flow and in fully mixed, free-stream turbulence. We artificially stiffened bumblebee wings *in vivo* by applying a micro-splint to the 1m-cu joint, which provides approximately 40% of the wing's overall flexibility in the chordwise direction (i.e., from leading to trailing edge; Mountcastle and Combes, 2013, Fig. 1). We hypothesized that bees with artificially stiffened wings would be less stable during flight, displaying greater body rotation rates.

2. Materials and methods

2.1. Study specimens

Bumblebee hives (*Bombus impatiens*) were acquired from an online distributor (Biobest) and maintained at room temperature in a large transparent enclosure. Bees had access to pollen grains in the surrounding enclosure and artificial nectar (50% sugar solution) within the hive, from which they could enter and exit as they pleased.

2.2. Training

We removed bees of average size (~180 mg) from the enclosure, cold-anesthetized them, and attached a triangular tag to the dorsal side of the thorax using cyanoacrylate glue. Tags were white with three black dots forming an isosceles triangle (2.7 x 2.3 mm), which served as visual landmarks for automated tracking and reconstruction of the bee's position and body orientation. We applied tags in a consistent location and orientation at the center of the thorax, such that the tag did not impede flight. Marker positions may have deviated slightly from the neutral axis of the bee, however the output variables we analyze (standard deviation of orientation and angular rotation rates) are unaffected by such offsets.

Tagged bees were isolated for approximately four hours without access to food, to improve their amenability to training using nectar rewards. After isolation, we provided the bee with a small amount of nectar and allowed it to feed for 5-10 seconds to stimulate its urge to forage, then placed it in the 90 x 40 x 50 cm working section of a 6-meter long suction-type wind tunnel (Fig. 1C). An artificial flower with a small nectar reward was placed at the upwind end of the working section.

Bees were initially introduced to the artificial flower and allowed to feed for a few seconds before being removed from the flower and placed at the downstream end of the wind tunnel. If the bee did not immediately fly back to the flower, it was captured and manually reintroduced. This procedure was repeated until the bee flew to the flower immediately after being released. Once bees were able to consistently find the artificial flower, the blue corolla of the artificial flower was removed to minimize airflow interference.

Not all bumblebees are amenable to training. Thus, bees were trained before the experimental treatments were applied to their wings. Once successfully trained, bees were cold-anesthetized again to begin the wing splinting process. Trained bees maintained consistent behavior after the splinting procedure, and did not need to be re-trained to locate the artificial flower within the wind tunnel.

2.3. Wing splinting

To experimentally stiffen bumblebee wings *in vivo*, we used a micro-splinting procedure developed by Mountcastle and Combes (2013), wherein a single piece of fine polyester glitter is applied to the dorsal surface of the wing, directly over the 1m-cu vein-joint, using UV adhesive (Fig. 1A). The mass of the glitter and adhesive together was approximately 5% of the total mass of the forewing (Mountcastle and Combes, 2013). To account for this addition of mass, we compared the flight performance of bees with artificially stiffened wings to their performance following a control treatment in which glitter was applied just adjacent to the 1m-cu joint (Fig. 1B), which adds the same

amount of mass at roughly the same position, but does not affect wing stiffness (Mountcastle and Combes, 2013).

For the wing-splinting procedure, bees were placed in a narrow brass tube with slits that allowed the wings to stick out while the body was braced. Immobilizing the bees in this way prevented them from injuring themselves by trying to escape, and protected their eyes from the UV light source used to cure the adhesive. To apply a splint to the wing, a single piece of glitter was first attached to a syringe tip with Crystalbond adhesive. The glittered syringe tip was then attached to a post connected to an x-y-z translational stage, which allowed precise alignment with either the 1m-cu vein-joint or the position of the control splint. A thin coat of UV-curable glue was applied to the bottom surface of the glitter, the syringe was lowered until the glitter contacted the wing, and a UV light source was used to quickly harden the UV-curable glue, affixing the glitter to the wing. The transparency of the wing membrane allowed the UV light to cure the adhesive from the opposite side of the wing.

After the UV glue was fully hardened (~30 seconds), a soldering iron was used to heat the metal syringe tip and melt the Crystalbond, releasing the adhesion between the syringe and the glitter - leaving the glitter attached to the wing. This procedure was then repeated on the other wing. Using this splinting technique on the 1m-cu joint, overall wing stiffness in the chordwise direction is increased by approximately 40%, whereas applying the splint to the control location does not increase stiffness (Mountcastle and Combes, 2013).

2.4. Flight trials

Each individual bee was flown in four conditions: artificially stiffened and control-splinted wings, in both laminar and turbulent airflow. We randomized the order of splinted and control-splinted treatments for each individual, and within each treatment we also randomized the order of laminar and turbulent flight trials. The turbulent flow was created by inserting a planar grid with 35 x 35-mm square openings 75 cm upwind of the working section of the wind tunnel (Fig. 1C). Airflow through the grid creates distinct vortices that break down to create fully mixed, free-stream turbulence in the working section of the wind tunnel. The turbulence intensity in the wind tunnel (standard deviation of flow velocity divided by mean flow velocity) was previously found to be 15% with the grid in place and <1.2% in the smooth flow condition (Ravi et al, 2015). The longitudinal integral length scale (the average size of the largest vortices produced) in the turbulent flow condition was approximately 40 mm, which is similar to the wing span of bumblebees. We adjusted the wind tunnel power so that the mean flow velocity was 2.5 m/s for both the laminar and turbulent conditions.

Flight sequences were filmed with four synchronized Photron SA3 high-speed cameras (San Diego, CA, USA) at 1,000 frames per second. At least 500 video frames were recorded for each treatment, and we captured data sets across all four treatments for 12 individual bees (for a total of 48 flight trials). For one bee, we also captured a series of higher frame-rate videos at 5,000 frames per second for each treatment, enabling us to resolve wing kinematics in detail and investigate how the splint affects wing shape throughout the stroke cycle.

2.5. Kinematic analysis

All data analysis was performed in MATLAB (R2014b; MathWorks). We used open-source MATLAB software (DLTdv5; Hedrick, 2008) to digitize the three points on the triangular tag on the thorax, and reconstruct the three-dimensional position and orientation of the bee's body during each flight trial using a direct linear transformation (Fig. 2A). Error in digitizing these points did not exceed 1-2 pixels, far less than the ~15 pixels separating each point on the tag. In the DLTdv5 software, each digitized frame returns a residual value – a metric of error – which is the root mean square pixel error in the 3D reconstruction of the points from the camera views. Residuals did not exceed 2 pixels for any of the sequences analyzed. To further estimate error, we compared the reconstructed distance between points to the actual physical distance (2.7 x 2.3 mm). The root mean square of this difference was < 0.04 mm, giving an uncertainty of < 2%.

The digitized data was initially processed with a 5^{th} order Butterworth low-pass filter with a cutoff frequency of 50 Hz to remove high-frequency digitizing jitter. We then fit a plane to the three body tag points and resolved the time history of body orientation in the three principal axes of roll, pitch and yaw using Euler angle rotations. (Fig. 2B).

To explore the effects of wing flexibility on flight stability, we examined two sets of kinematic parameters: the standard deviations of body orientations and the mean, absolute rotation rates. Prior to calculating the standard deviations of body roll, pitch and yaw, we first processed the body position data with a 5^{th} order Butterworth high-pass filter with a cutoff frequency of 10 Hz in order to exclude low-frequency components of

body motion that may be associated with voluntary changes in flight trajectory (Ravi et al, 2013; Mountcastle et al, 2015). Roll, pitch and yaw rotation rates were calculated by numerically differentiating the body orientations over time, then making a final adjustment to these angular velocities to account for the fact that they do not form an orthogonal set (after Ravi et. al, 2013). We compared both sets of kinematic parameters for bees with control-splinted vs. experimentally stiffened wings using two-tailed paired t-tests, performing separate comparisons for turbulent and smooth flow conditions.

To test whether bees were actively changing their flight behavior as a result of wing splinting or flow condition, we examined the low frequency motions of their flight path trajectories, which are associated with voluntary steering activity (Ravi et al., 2013). We applied a 5^{th} order Butterworth low-pass filter to the data with a 10-Hz cutoff frequency, and added the mean wind tunnel flow velocity, integrated over time, to the component of distance travelled upwind. We calculated median turning rate and median curvature of the bee's flight path (as in Combes et al., 2012), and calculated path sinuosity of each flight by dividing the total length of the flight path by the straight-line distance between the start and end points of the trial. Two-tailed paired t-tests were performed to compare each metric between splinted and unsplinted trials in laminar and turbulent airflows.

Additionally, we measured wingbeat frequency to verify that bees do not change their gross wing kinematics when flapping with control splints vs. experimental splints (as in Mountcastle and Combes, 2013). To calculate average wingbeat frequency, we counted the number of wing strokes completed in each flight trial and divided by the trial

duration. Wingbeat frequency was compared between splinted and control-splinted trials using two-tailed paired t-tests.

Finally, to measure how wing stiffening changed the projected wing area and to model the associated effects on wing drag, we digitized wing kinematics in the four video sequences that were captured at the higher frame-rate (5,000 Hz). For each trial, we digitized four points on the right forewing across 11 consecutive wing strokes: the wing base, the stigma (along the leading edge), the wing tip, and the notch where the forewing and hindwing meet along the trailing edge (Fig. 4A). The digitized data were processed with a 5^{th} order Butterworth low-pass filter with a cutoff frequency of 1000 Hz to remove higher-frequency digitizing jitter.

Instantaneous wing velocity was calculated for the nominal center of the wing (defined as the midpoint between the leading edge stigma and the trailing edge notch), which incorporated both the rotational motions of the flapping wing and the rectilinear flow velocity in the wind tunnel. We approximated forewing area as the area enclosed by the four tracked wing points, and calculated its projection onto the plane normal to the instantaneous velocity vector. Drag force on the wing can be expressed in a generalized form by the equation:

$$F_D = 0.5\,\rho\,v^2\,C_d\,A, \qquad (1)$$

where ρ is fluid density, v is the wing's velocity, C_d is coefficient of drag, and A is the projected wing area. Although we cannot offer an explicit solution to the drag equation in this case, since the value of C_d is unknown, we can calculate the product of wing area and

velocity squared ($A*v^2$), which is proportional to the drag force, and compare this value between wing treatments.

We calculated the gross wing sweep position and the time-varying values: A, v^2, and their product $A*v^2$, throughout all 11 wing strokes for each treatment. We then divided the data into discrete wing strokes based on wing sweep position, and normalized strokes by resampling onto a uniform time vector (equal to the average length of a wingstroke). Finally, we found the average A, v^2, and $A*v^2$ values for each wingstroke (Fig. 4C), and used Wilcoxon signed-rank tests to assess whether mean ranks differed between the splinted and flexible groups, in both laminar and turbulent conditions.

3. Results

3.1. Body stability

Artificially stiffening the wings caused a significant increase in both the standard deviation about the roll axis (p=0.005) and mean rotation rate about the roll axis in laminar airflow (p=0.026; two-tailed paired t-tests; n=12; Fig. 3). Wing stiffening caused roll standard deviations to increase by 26% on average, from 2.14 ± 0.49 deg. to 2.70 ± 0.51 deg., and mean roll rates to increase by 17% on average, from 325 ± 80 deg/s to 381 ± 82 deg/s. In contrast, we found no significant differences in either standard deviations or rotation rates about the pitch (standard deviation, σ: p=0.64; rotation rate, ω: p=0.75) or yaw (σ: p=0.14; ω: p=0.054; two-tailed paired t-tests; n=12) axes between the two wing treatment groups in laminar flow, though yaw rates were approaching significance. In general, roll rates were substantially higher than pitch or yaw rates in laminar flow (Fig. 3), confirming previous findings that bees are least stable around the roll axis (Ravi et al., 2013; Mountcastle et al., 2015). In turbulent airflow, we found no significant differences in standard deviations or rotation rates about any body axis (σ roll: p=0.74; σ pitch: p=0.11; σ yaw: p=0.80; ω roll: p=0.57; ω pitch: p=0.15; ω yaw: p=0.36; two-tailed paired t-tests; n=12).

3.3. Behavioral changes

When examining only the low-frequency casting motions that are associated primarily with active flight maneuvers, we found significant differences between bees with stiffened and flexible wings, but only in the turbulent flow condition (Fig. 5). Bees flying with splinted wings in turbulent flow displayed significantly higher median turning

rate, median path curvature, and log(sinuosity) (p = 0.017, 0.024, and 0.02, respectively; two-tailed paired t-tests, n = 12). Wing stiffening caused median turning rate to increase from 33.6±6.5 deg/s to 44.3 ± 11.6 deg/s, median path curvature to increase from 23.7 ± 4.5 cm to 30.7 ± 7.9 cm, and log(sinuosity) to increase from 3.47 ± 1.14e-4 to 6.67 ± 4.27e-4 (Fig. 5).

3.4. Wing kinematics

The mean wingbeat frequency across all trials was 159 ± 11 Hz, and there was no significant difference in wingbeat frequency between splinted and control-splinted wing treatments, in either laminar or turbulent airflow (laminar $p = 0.74$; turbulent $p = 0.67$; two-tailed paired t-tests, n = 12).

Based on analysis of the high frame-rate video sequences, wing stroke amplitude of bees flying in laminar airflow decreased by 26% with wing stiffening, from an average of 124 ± 5° in control-splinted trials to 99 ± 7° in splinted trials ($p = .001$; Wilcoxon signed-rank test, n=11 wingstrokes). There was no significant difference in stroke amplitude between wing treatments in the turbulent condition, which was 95 ± 7° for the control-splinted group and 95 ± 5° for the splinted group ($p = 0.97$; Wilcoxon signed-rank test; n=11).

In both flow conditions, we found significantly higher stroke-averaged values of $A*v^2$ (proportional to wing drag) for splinted wings as compared to flexible wings (laminar: $p = 0.01$; turbulent: $p = 0.001$; Wilcoxon signed-rank test, n=11; Fig 4). $A*v^2$ increased by 38%, from 1.41 $x10^4$ ± 1.3 $x10^3$ cm^4/s^2 to 1.95$x10^4$ ± 5.5 $x10^3$ cm^4/s^2 in laminar flow, and by 54%, from 1.40 $x10^4$ ± 2.1 $x10^3$ cm^4/s^2 to 2.15 $x10^4$ ± 3.6 $x10^3$

cm^4/s^2 in turbulent flow. This increase can be explained in the laminar condition by a 45% increase in the projected wing area caused by splinting (p = 0.001), while stroke-averaged v^2 did not change significantly (p = 0.70; Wilcoxon signed-rank tests; n=11; Fig. 4). In the turbulent condition, on the other hand, both projected wing area and v^2 increased with splinting, by 20% and 25% respectively (wing area: p = 0.01; v^2: p = 0.01; Wilcoxon signed-rank tests; n=11). However, wing velocity predictions in turbulence should be viewed with caution, as we cannot accurately account for local flow variations experienced by the wings in unpredictable, turbulent flow.

4. Discussion

We found that artificially increasing bumblebee wing stiffness causes a significant reduction in flight stability during forward flight in laminar airflow, as demonstrated by an increase in both the standard deviation of roll angle and roll rates. Consistent with prior studies (Ravi at al., 2013, Mountcastle et al. 2015), we found that body rotation rates were highest about the roll axis in both airflow conditions (Fig. 4). Because moment of inertia is lowest around the roll axis, bees are able to initiate rolling maneuvers easily, but they are also least stable to external perturbations around this axis (Mountcastle et al. 2015). Accordingly, bees displayed higher rolling rates in turbulent air than in laminar air, regardless of wing treatment. Interestingly, though, rolling rates in turbulent airflow increased only slightly with wing stiffening, and this increase was not statistically significant, whereas wing stiffening did lead to significantly higher rolling rates in laminar airflow (Fig. 4).

Stiffening bumblebee wings by immobilizing the 1m-cu joint has previously been shown to increase chordwise flexural stiffness by approximately 40%, reducing dynamic changes in wing concavity (i.e., camber or cupping) that normally occur during the stroke cycle, particularly during ventral stroke reversal (Mountcastle and Combes, 2013). However, the aerodynamic mechanism(s) that underlie greater force production by flexible wings during ventral stroke reversal remain unclear, and the extent to which this phenomenon may be implicated in flight stability is unknown. On the other hand, we can speculate on a different mechanism by which stiffened wings may be decreasing flight stability in this study.

Body rotations can be driven by any type of force asymmetry between the left and right sides of the body. These asymmetries may be generated by the bee's self-motions,

for example by intentional or unintentional differences in flapping kinematics between the left and right wings, or by flying with a body orientation that is not aligned to the oncoming flow (i.e., yawed to the left or right), causing the two wings to experience different flow conditions. Force asymmetries may also arise from unpredictable airflow asymmetries between the left and right wings, caused by turbulence or wind gusts for example. Regardless of how they are generated, flow asymmetries between the left and right wings can lead to asymmetries in both lift and drag production. Mountcastle and Combes (2013) found that wing splinting actually decreased vertical force production during hovering flight, suggesting that drag (rather than lift, which presumably decreases with wing stiffening) may be the primary mechanism by which wing stiffening causes instabilities around the rolling axis during forward flight.

We therefore explored the possibility that splinted wings experience greater drag forces due to a larger projected surface area, which we hypothesize would amplify any aerodynamic force asymmetry on the wings and thereby generate greater body torques. Indeed, we found that splinted wings presented a greater projected area into the oncoming flow, with a concomitant increase in the product of wing area and velocity squared ($A*v^2$), which is proportional to drag force. The effect of wing splinting on drag is particularly evident during the downstroke and ventral stroke reversal (Fig. 5E). This proposed explanation is consistent with prior studies that have shown that wing flexibility decreases drag (Miller and Peskin, 2009; Zhao et al. 2009). Thus, even though wing splinting may have the most noticeable effect on wing shape during ventral stroke reversal (Mountcastle and Combes, 2013), the effects on drag appear to be most pronounced during the downstroke, due to the wing's high velocity during this phase of the stroke cycle – velocity that is further amplified during forward flight.

If an increase in wing drag caused by splinting is responsible for higher roll deviations and rotation rates in laminar airflow, why then do bees with stiffened wings not experience a similar destabilizing effect in turbulence (Fig. 4)? Although our study cannot answer this question definitively, we can speculate on two potential factors that may help explain this surprising null result, both of which are related to the higher overall rotation rates observed in turbulence as compared to laminar flow. First, our data suggests that bees change their flight behavior significantly when flying with splinted wings in turbulence. When considering only the low frequency movements associated with active steering behavior, we found that bees with stiffened wings displayed significantly higher average median turning rates, flight path curvature, and sinuosity in turbulent airflow. However, these turning metrics were all similar for bees flying in laminar air (with flexible or stiffened wings) and in turbulence with flexible wings. Together, these results suggest that bees in laminar airflow do not need to adjust their flight behavior to cope with the increased body rotation rates caused by wing splinting, whereas the generally higher rotation rates imposed by turbulence (Fig. 4) may bring bees to a threshold for instability tolerance, after which they display a behavioral change to avoid experiencing further instability caused by wing splinting.

The second potential explanation for the lack of a significant effect of wing stiffening in turbulent air is that the higher instabilities imposed by turbulent airflow (as compared to laminar flow) may wash out the relatively smaller effects of wing splinting on stability. As Fig. 4 illustrates, roll rates do increase moderately in bees flying with stiffened wings in turbulent flow, hinting at a possible effect, even though we didn't find this difference to be statistically significant. The greater magnitude of externally imposed instabilities and random nature of turbulent flow may necessitate a larger sample size to

help clarify whether wing splinting does in fact decrease stability in turbulence, as it does in laminar flow.

This is the first study of its kind to examine the effects of wing flexibility on forward flight stability in insects. Over the past decade, there has been a steadily growing body of work focused on understanding the role of wing flexibility in flight performance, and the majority of these studies have revealed that passive wing deformations can enhance aerodynamic force and/or efficiency. In this study, we have shown that wing flexibility can also increase flight stability during forward flight, a result that will be of interest to biologists studying animal flight aerodynamics, wing functional morphology, and evolution, as well as to engineers seeking to build flapping micro air vehicles capable of stable flight in the natural world.

Competing interests

The authors declare no competing interests.

Authors' contributions

E.A.M. carried out data collection and analyses, and drafted the manuscript. A.M.M. and S.A.C. performed data analyses. All authors participated in the design of the study, drafting of the manuscript, and gave final approval for publication.

Acknowledgements

The authors would like to thank Callin Switzer for advice on statistical analysis.

Funding

This work was supported by National Science Foundation grants IOS-1253677 and CCF-0926158 to S.A.C., and by Harvard College Research Program and Museum of Comparative Zoology Grants in Aid of Undergraduate Research to E.A.M.

Figures

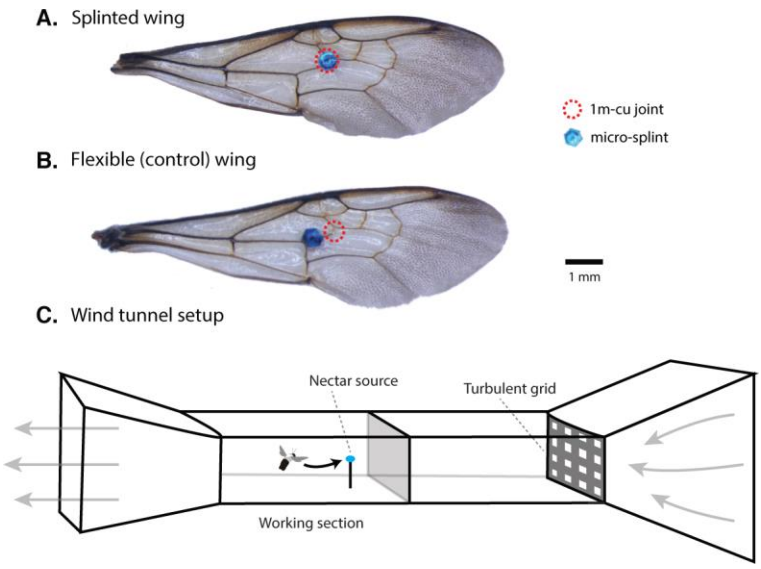

Figure 1. Wing splint treatments and wind tunnel setup. (A) Experimental micro-splint treatment: a single piece of polyester glitter (blue, 0.44 mm diameter, 20 μg) was attached to the 1m-cu joint on both forewings in order to increase wing stiffness in the chordwise direction. (B) Control treatment: the glitter was attached just adjacent to the 1m-cu joint, adding the same mass to each wing but allowing the joint to flex naturally during flapping flight. (C) Wind tunnel with 90 x 40 x 50- cm working section, in which bees flew to a nectar source at the upwind end. The turbulence-generating planar grid was placed upwind of the working section, and mean flow was set to 2.5 m/s.

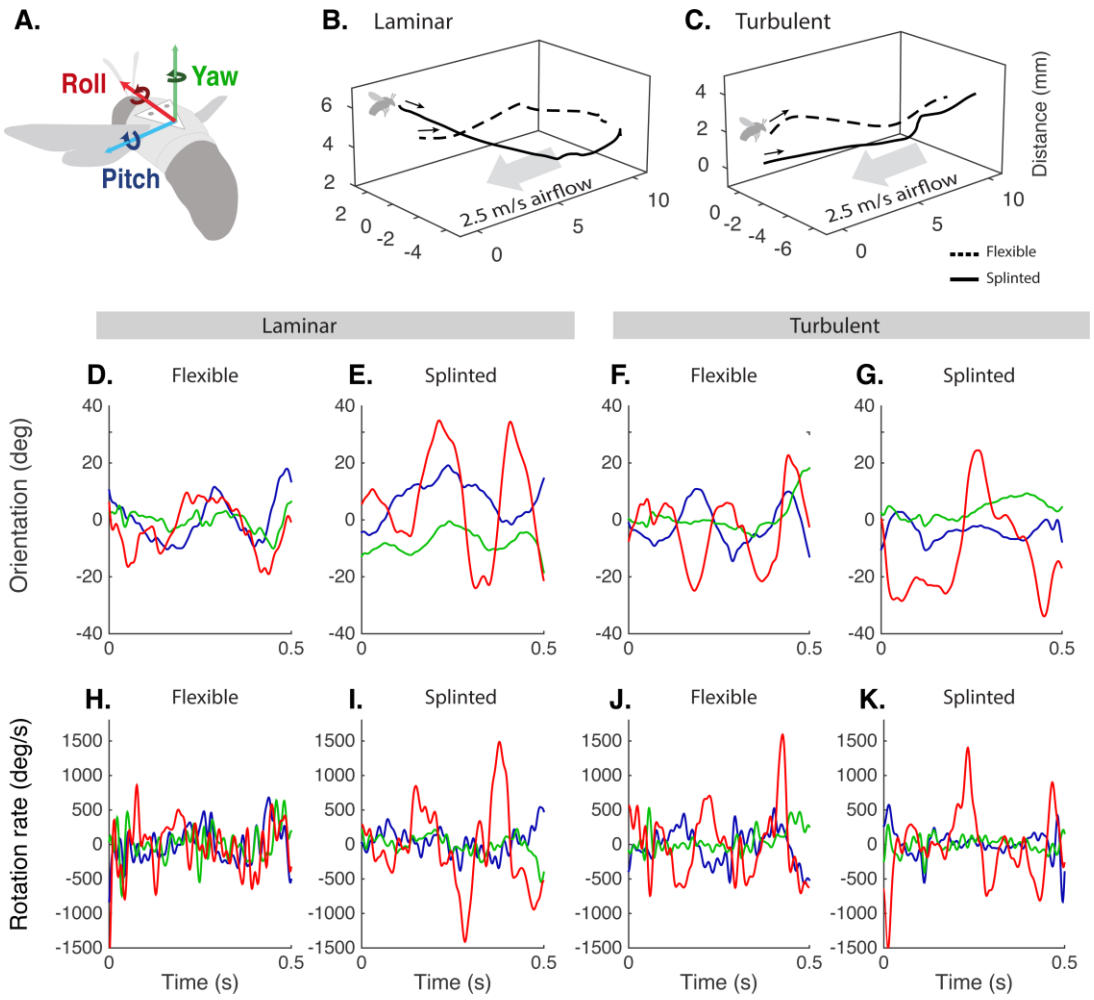

Figure 2. Representative flight trials and associated kinematic data. (A) Bee body coordinate system used in our analysis, showing the colors used to represent motions around these axes in the graphs below. (B-C) Three-dimensional flight trajectories in the wind tunnel, in laminar and turbulent flow. (D-G). Instantaneous body orientation angles and (H-K) rotation rates during a 0.5-sec. segment of the associated flight trajectory, for each of the four treatments (panels from left to right: flexible laminar, splinted laminar, flexible turbulent, splinted turbulent). Roll is shown in red, yaw in green, and pitch in blue, as in A.

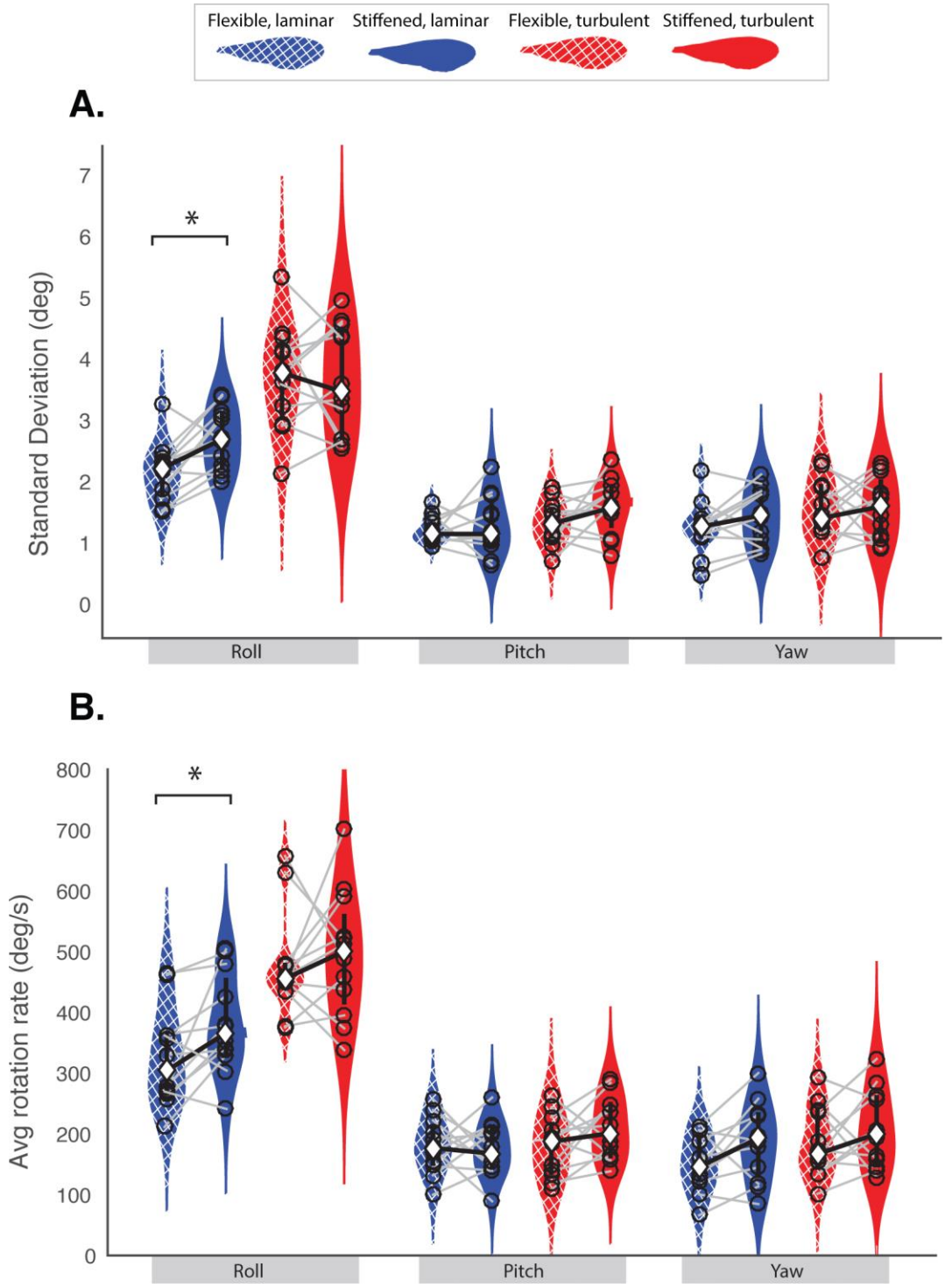
Flexible, laminar
Stiffened, laminar
Flexible, turbulent
Stiffened, turbulent
A.
Standard Deviation (deg)
0
1
2
3
4
5
6
7
*
Roll
Pitch
Yaw
B.
Avg rotation rate (deg/s)
0
100
200
300
400
500
600
700
800
*
Roll
Pitch
Yaw

Figure 3. (A) Average standard deviations of roll, pitch, and yaw, and (B) average rotation rates around these axes, for bumblebees flying in laminar and turbulent airflow (n=12 trials per treatment). Bees with artificially stiffened wings displayed significantly higher roll standard deviations and rotation rates in laminar airflow (indicated by an asterisk). The width of each violin plot represents density probability, grey lines between treatments connect paired trials performed on the same individual, and white diamonds represent the mean.

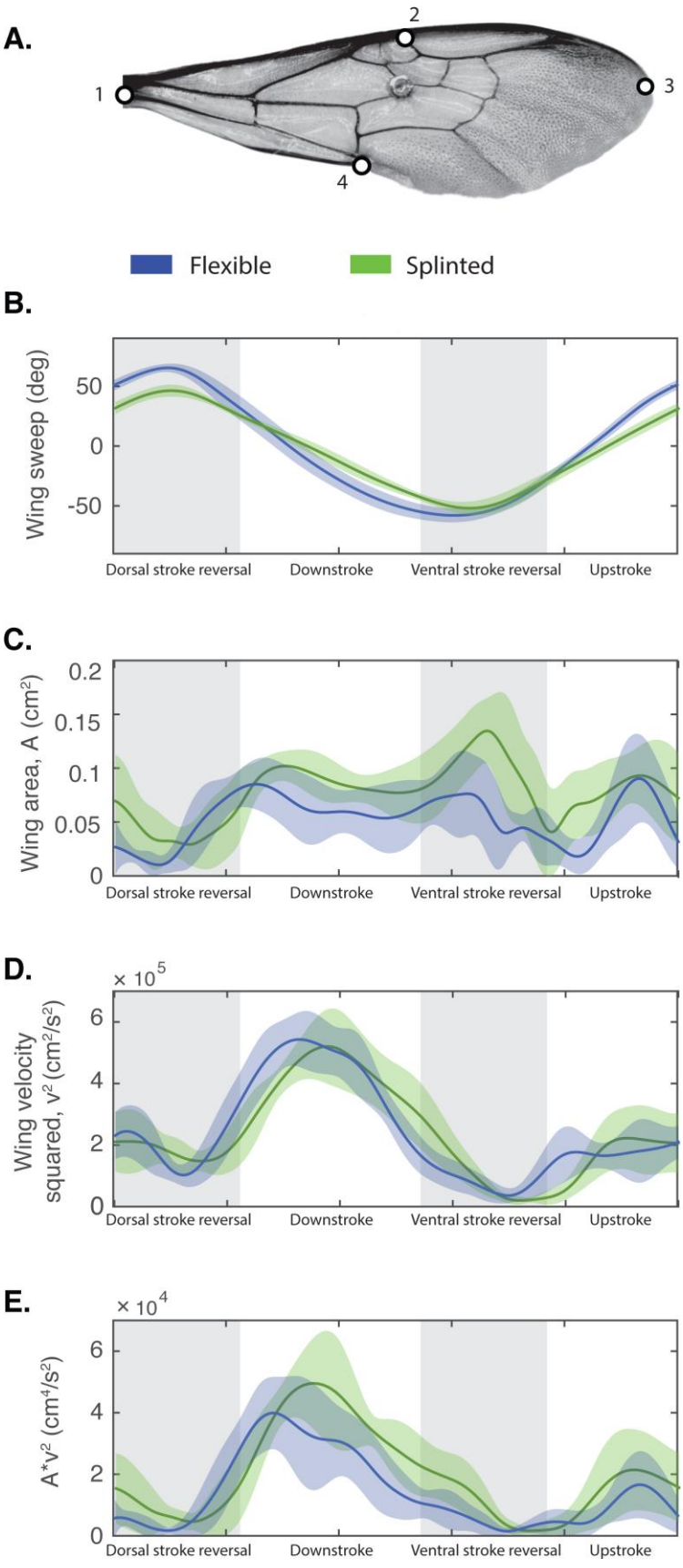

Journal of Experimental Biology • Advance article

Figure 4. Wing kinematic data from bumblebee flight trials in laminar airflow, with splinted and flexible wings. (A) Four points on the wing were digitized to estimate wing area. (B*)* Wing sweep position over eleven consecutive strokes for each wing treatment, normalized to the same stroke period and pooled. Dark line represents average wing sweep, and lighter bands show standard deviation. (C) Projected wing area, A, (D) wing velocity squared, v^2, and (E) product of projected wing area and wing velocity squared, $A*v^2$, (proportional to drag) throughout the wingbeat cycle for the strokes shown in (B).

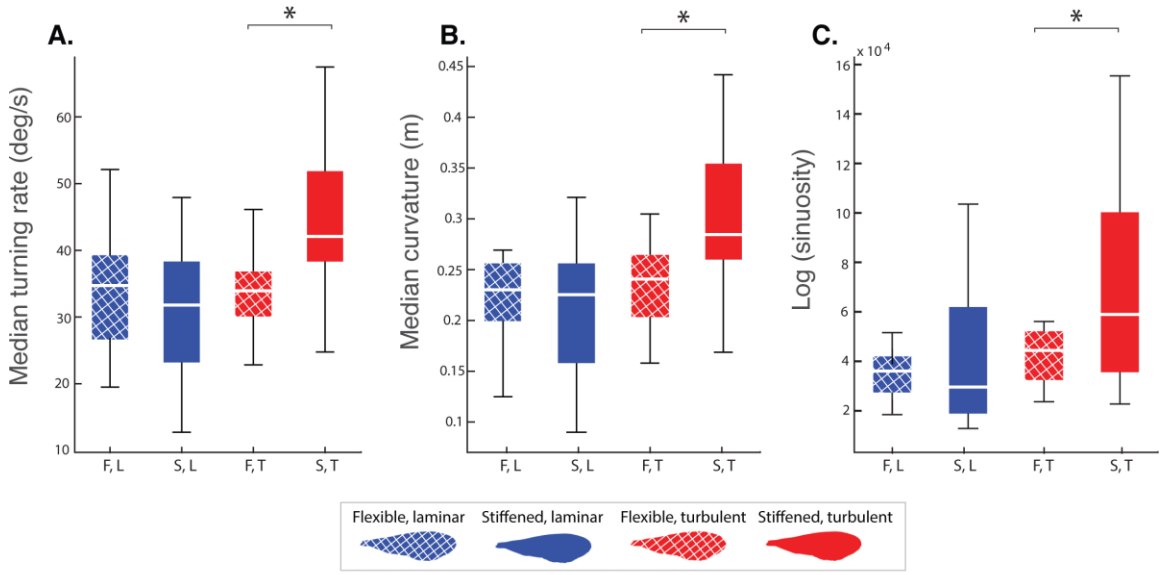

Figure 5. Median turning rate, median curvature, and log(sinuosity) of low-frequency (<10 Hz) movements for all flight trials (n=12 trials per treatment). Bees with splinted wings in turbulent airflow displayed significantly higher median turning rate, median curvature, and sinuosity than bees with flexible wings, or bees in laminar flow (with either wing condition). Box and whisker plots show the median, quartiles, and range of data points, with outliers plotted as plus signs. Asterisks indicate a significant difference.

References

Combes S.A., Rundle D.E., Iwsaki J.M., and Crall, J.D. (2012). Linking biomechanics and ecology through predator-prey interactions: Flight performance of dragonflies and their prey. *J. Exp. Biol*. **215**, 903-913.

Daniel T.L. and Combes S.A. (2002). Flexible wings and fins: bending by inertial or fluid dynamic forces? *Integr. Comp Biol.* **42**, 1044-1049.

Du G. and Sun M. (2010). Effects of wing deformation on aerodynamic forces in hovering hoverflies. *J. Exp. Biol.* **213**, 2273-2283.

Hedrick T.L. (2008). Software techniques for two- and three-dimensional kinematic measurements of biological and biomimetic systems. *Bioinspir. Biomim.* **3**, 034001.

Heinrich B. (2004). *Bumblebee Economics.* Cambridge, MA. Harvard University Press.

Kim D.K., Han J.H., and Kwon K.J. (2009). Wind tunnel tests for a flapping wing model with a changeable camber using macro-fiber composite actuators. *Smart Mater. Struct.* **18**, 024008.

Miller L.A. and Peskin C.S. (2009). Flexible clap and fling in tiny insect flight. *J. Exp. Biol.* **212**, 3076-3090.

Mountcastle A.M. and Combes S.A. (2013). Wing flexibility enhances load-lifting capacity in bumblebees. *Proc. Roy. Soc. B.* **208**, 20130531.

Mountcastle A.M. and Combes S.A. (2014). Biomechanical strategies for mitigating collision damage in insect wings: structural design versus embedded elastic materials. *J. Exp. Biol.* **217**, 1108-1115.

Mountcastle A.M., Ravi S,. and Combes S.A. (2015). Nectar vs. pollen loading affects the trade-off between flight stability and maneuverability in bumblebees. *Proc Natl Acad Sci* **112**, 10527–10532.

Nakata T. and Liu H. (2012). Aerodynamic performance of a hovering hawkmoth with flexible wings: a computational approach. *Proc. Roy. Soc. B.* **279**, 722-731.

Ortega-Jimenez V.M., Greeter J.S.M., Mittal R., and Hedrick T.L. (2013). Hawkmoth flight stability in turbulent vortex streets. *J. Exp. Biol.* **216**, 4567-4579.

Ortega-Jimenez V.M., Sapir N., Wolf M., Variano E.A., and Dudley R. (2014). Into turbulent air: size-dependent effects of von Karman vortex streets on hummingbird flight kinematics and energetics. *Proc. R. Soc. B.* **281**, 20140180.

Ravi S., Crall J.D., Fisher A., and Combes S.A. (2013). Rolling with the flow: bumblebees flying in unsteady wakes. *J. Exp. Biol.* **216**, 4299-4309

Ravi S., Crall, J.D., McNeilly L., Gagliardi S.F., Biewener A.A., Combes SA. (2015). Hummingbird flight stability and control in freestream turbulent winds. *J. Exp. Biol.* **218**, 1444-1452.

Reynolds K.V., Thomas A.R., Taylor G.K. (2014). Wing tucks are a response to atmospheric turbulence in the soaring flight of the steppe eagle Aquila nipalensis. *J. R. Soc. Interface.* **11**, 20140645.

Shyy W. et al. (2008). Computational aerodynamics of low Reynolds number plunging, pitching and flexible wings for MAV applications. *Acta Mech. Sinica* **24**, 351 –373.

Srinivasan M.V. and Zhang S. (2004). Visual motor computations in insects. *Annu. Rev. Neurosci.* **27.** 679-696.

Stull R.B. (1988). An Introduction to Boundary Layer Meteorology. Dordrecht: Kluwer Academic Publishers.

Weis-Fogh T. (1961). Thermodynamic properties of resilin, a rubber-like protein. *J. Mol. Biol.* **3**, 520-531.

Wootton R.J. (1992). Functional morphology of insect wings. *Ann. Rev. Entomology*. 37:113-140.

Young J., Walker S.M., Bomphrey R.J., Taylor G.K. and Thomas A.L.R. (2009). Details of insect wing design and deformation enhance aerodynamic function and flight efficiency. *Science* **325**, 1549-1552.

Zhao L., Huang Q., Deng X., and Sane S. (2009). The effect of chord-wise flexibility on the aerodynamic force generation of flapping wings: experimental studies. *IEEE Trans. Robot. Autom.* 4207-4212.